2. N. Ibl, Ph. Javet, and F. Stahel, *Electrochim. Acta*, **17**, 733 (1972).
3. J. L. Barton and J. O'M. Bockris, *Proc. R. Soc. London, Ser. A*, **268**, 485 (1962).
4. D. R. Hamilton, *Electrochim. Acta*, **8**, 731 (1963).
5. J. W. Diggle, A. R. Despic, and J. O'M. Bockris, *This Journal*, **116**, 1503 (1969).
6. Y. Oren and U. Landau, *Electrochim. Acta*, **27**, 739 (1982).
7. K. I. Popov, L. J. M. Djukie, M. G. Pavlovie, and M. D. Maksimovic, *J. Appl. Electrochem.*, **9**, 527 (1979).
8. K. I. Popov, M. D. Maksimovic, and P. T. Lukic, *ibid.*, **10**, 299 (1980).
9. K. I. Popov, M. D. Maksimovic, J. D. Trnjancev, and M. G. Pavlovic, *ibid.*, **11**, 239 (1981).
10. K. I. Popov, Z. P. Rodaljevic, N. V. Kristajic, and S. R. Popov, *Surf. Tech.*, **23**, 167 (1984).
11. U. Landau, EPRI Report EM-2393, EPRI, Research Reports Center, Palo Alto, CA (1982).
12. W. W. Mullins and R. F. Sekerka, *J. Appl. Phys.*, **34**, 323 (1963).
13. C. Wagner, *This Journal*, **101**, 225 (1954).
14. P. Fedkiw, *ibid.*, **127**, 1304 (1980).
15. G. A. Prentice and C. W. Tobias, *ibid.*, **129**, 316 (1982).
16. J. A. Mcgeough and H. Rasmussen, *J. Mech. Eng. Sci.*, **18**, 271 (1976).
17. J. A. Mcgeough and H. Rasmussen, *ibid.*, **19**, 163 (1977).
18. J. A. Mcgeough and H. Rasmussen, *ibid.*, **23**, 114 (1981).
19. R. Aogaki, K. Kitazawa, Y. Kōse, and K. Fukei, *Electrochim. Acta*, **25**, 965 (1980).
20. R. Aogaki and T. Makino, *ibid.*, **26**, 1509 (1981).
21. R. Aogaki, *This Journal*, **129**, 2442 (1982).
22. R. Aogaki, *ibid.*, **129**, 2447 (1982).
23. R. Aogaki and T. Makino, *ibid.*, **131**, 40 (1984).
24. R. F. Sekerka, *J. Appl. Phys.*, **36**, 265 (1965).
25. S. R. Coriell and S. C. Hardy, *ibid.*, **40**, 1652 (1969).

A Solid-State Thin Film Cell for *In Situ* Transmission Electron Microscopy of Electrodeposited Silver on Gold

K. J. Hanson,* J. M. Gibson, and M. L. McDonald

AT&T Bell Laboratories, Murray Hill, New Jersey 07974

ABSTRACT

A cell to permit *in situ* imaging of the electrodeposition of silver on gold <100> from a polymer electrolyte by TEM is described. The extremely thin electrochemical cells were composed of a layer of polyethylene oxide containing a silver salt between evaporated silver and gold electrodes. Cyclic voltammetry experiments in larger cells show the deposition and stripping behavior of silver on polycrystalline gold from the polymer electrolyte as a function of temperature. Observations in preliminary *in situ* TEM experiments include the nucleation and growth, and coalescence of silver islands oriented epitaxially to the gold electrode.

Surface science has developed to allow chemical and structural analysis on the monolayer level to be routinely obtained. Such studies are however almost exclusively limited to vacuum-solid interfaces and so can give insight into crystal growth from the vapor phase, but permit no direct studies of electrodeposition. As a result of this limitation, *ex situ* studies of electrodeposited layers using transmission or scanning electron microscopy have been used to gain an understanding of the nucleation and growth processes of electrodeposition (1). With the use of a solid electrolyte, a sufficiently thin cell could be operated in the vacuum chamber of a transmission electron microscope to provide an *in situ* method for studying the initial stages of electrodeposition. Recently, ionically conducting polymers have been developed as solid electrolytes for battery applications (2, 3) which show sufficient conductivities ($\sim 10^{-4}\ \Omega^{-1}\text{cm}^{-1}$) at low temperatures (60°C) to permit their use as a solid electrolyte in vacuum. In this paper we report preliminary results from our study of the electrochemical deposition of silver onto a gold <100> surface in a Au/PEO(Ag^+)/Ag thin film cell observed *in situ* in a transmission electron microscope.

Approach

The deposition of silver on gold was chosen as a model system in this study to make use of established techniques for making and characterizing thin films by evaporation and because the small lattice mismatch between silver and gold (0.17%) would lead to epitaxial deposits. In addition, the electrode films could be oriented by choosing an appropriate substrate and carefully controlling the growth conditions in the chamber. By orienting at least one of the films, it is possible to distinguish the metal layers in the diffraction pattern of the total cell.

The electrodeposition of silver on gold substrates has been studied by Bruckenstein and co-workers (4-6) from $Ag^+/HClO_4$ aqueous solutions. They found that underpotential deposited silver on polycrystalline gold exhibited only one deposition peak in the potentiodynamic response. Rao and Weil (7, 8) have studied the electrodeposition of gold on polycrystalline silver from an alkaline sulfite solution by thinning the silver electrode after deposition and using TEM to observe the deposited layer. They conclude that the initial structure of the epitaxial gold deposit is three-dimensional crystallites. Unfortunately, the deposition of silver on gold could not be studied in this way because the gold electrode could not be thinned without disturbing the silver deposit. Few studies have described the electrodeposition of metals other than lithium from polymer electrolytes. We have therefore performed preliminary experiments to determine the conditions and compositions under which silver would deposit from a PEO-based electrolyte.

Electrochemistry

The electrochemical cells used in the preliminary experiments were prepared in a glove box containing a dry argon atmosphere to prevent decomposition of the salts. The electrodes were 3 mm diameter disks of 0.025 mm thick gold (99.99%, Alfa) and silver (99.9%, Alfa) foils. The disks were punched out between pieces of filter paper or cut out with a circular bore, and cleaned by rinsing in dry acetone and acetonitrile. The salts used in this study, $AgAsF_6$ (Alfa), $AgBF_4$ (Alfa), were reagent grade and dried in a vacuum oven prior to use or recrystallized in the glove box. Acetonitrile (Aldrich, anhydrous) was used as received. The electrolyte films for the preliminary experiments were prepared by casting an acetonitrile solution of the salt and polyethylene oxide (Aldrich Chemical, MW 10,000) on a PTFE plate and allowing the solvent to evaporate inside the glove box; the films were approximately 25 μm thick. Samples were removed from the casting plate and cut into 3 mm disks using a bore cutter.

The electrochemical cells were assembled by inserting a trilayer disk of silver foil, PEO-salt electrolyte, and a gold

* Electrochemical Society Active Member.

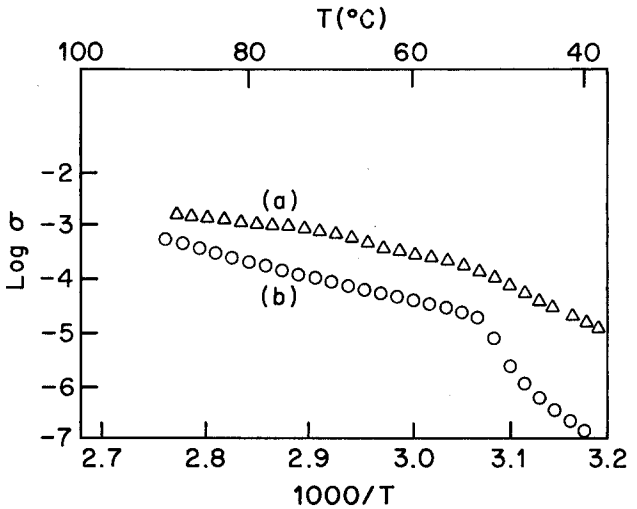

Fig. 1. Arrhenius plot of log conductivity ($\Omega^{-1}cm^{-1}$) vs. 1000/T (K^{-1}) for polyethylene oxide complexes of (a) $AgBF_4$ and (b) $AgAsF_6$.

foil into the center of a 1/8 in. PTFE Swagelok (copyright) union which had been drilled out to have straight sides. Stainless steel 1/4 in. rods were inserted on each side of the union to make electrical contacts. In each case, the gold was the working electrode, and silver the counter and reference electrode.

Electrochemical measurements were made with a digital potentiostat (PAR Model 173). The cells were tested at room temperature in the glove box or removed to a thermostatically controlled oven (Ramsco, Incorporated).

Conductivity measurements were made by loading a small sample of the cast polymer/salt film into a ceramic die. Stainless steel screws having polished ends were inserted into the die and tightened against the film. The temperature of the loaded die was controlled in a nitrogen-purged furnace. Complex impedance measurements were made every 2-3 degrees between 30° and 130°C. A complete description of the apparatus for the conductivity measurements is given by Kaplan *et al.* (9).

Results.—Figure 1 shows the conductivity of PEO/$AgAsF_6$ (10 PEO monomers per Ag^+) as a function of temperature. The results for the same concentration of $AgBF_4$ are included for comparison. The behavior of the conductivity of $AgAsF_6$ as a function of temperature shows the same functional relationship as the other silver salts-PEO electrolytes, following an Arrhenius relationship with a discontinuity near the melting point of crystalline PEO.

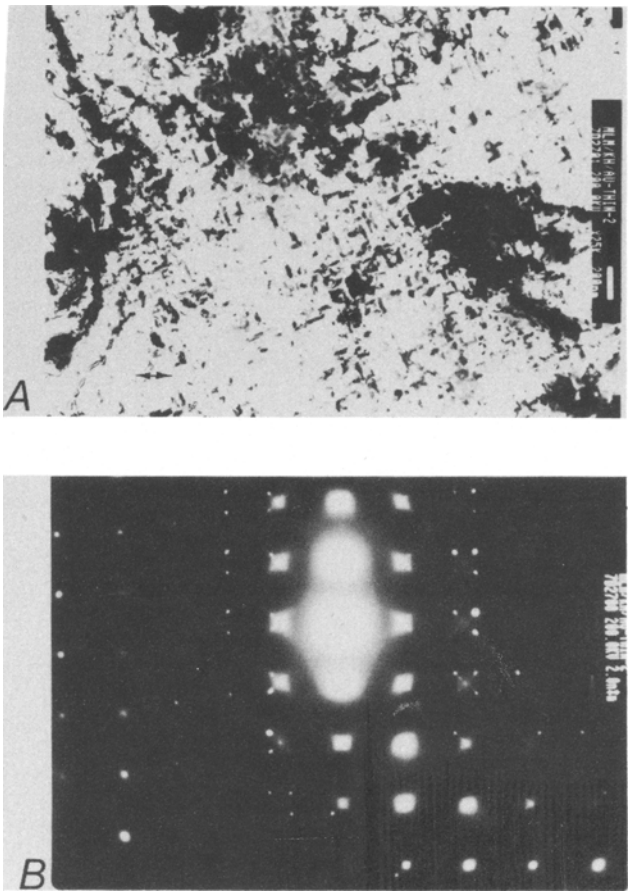

Fig. 3 TEM image (A) and diffraction pattern (B) of a 350Å gold film.

The poor conductivity of the polymer electrolyte at low temperatures profoundly affects the behavior of the cyclic voltammograms (CV) observed in the metal foil cells. Figure 2 shows voltammograms taken at 22°, 34°, 42°, and 59°C. In each case, the sweep was initiated at 0 V (*vs.* the silver counterelectrode), and the potential was swept first in the

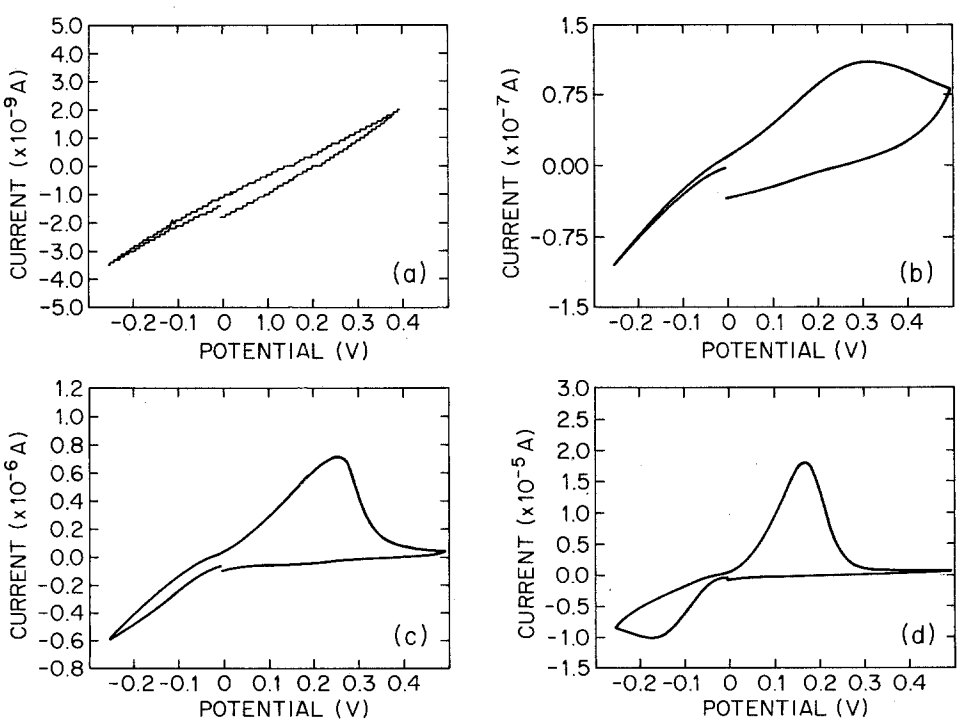

Fig. 2. Cyclic voltammograms of $AgAsF_6$ in PEO at various temperatures. In each case the sweep was from 0 V (*vs.* the silver counterelectrode) to −250 mV to 500 mV to 0 mV at a sweep rate of 10 mV/s. (a) 22°C, (b) 33°C, (c) 42°C, and (d) 59°C.

cathodic, then in the anodic direction at a rate of 10 mV/s. At room temperature, the behavior is dominated by the ohmic drop in the cell and the shape of the CV curve resembles the behavior of a simple resistor. As the temperature is increased, the faradaic current from silver deposition and dissolution becomes a larger fraction of the total current and the voltammogram approaches the shape given by theory for metal that is reversibly deposited and stripped on a dissimilar substrate (10).

TEM Experiments

The cell for *in situ* TEM is similar to the cell described above but it is about 1000 times thinner. The anode and cathode are thin silver and gold films; they are separated by a layer of polyethylene oxide containing the silver salt. In order for satisfactory images to be formed it is desirable for the cell thickness to be of order 1500Å or less; this requirement limited the metal films to approximately 300-600Å. The electrodes were made by vacuum evaporation, following the methods of Adamsky and LeBlanc (11), Mathews (12), and Pashley (13). Oriented gold films were made by evaporating gold from an alumina crucible onto freshly cleaved epitaxial quality NaCl rock salt crystals which were heated to 400°C in an evacuated (10^{-6} torr) bell jar. The gold thickness during evaporation was monitored by a quartz crystal oscillator. During evaporation, a mica mask was held between the salt surface and the gold source to produce a pattern of circles of gold on the salt surface.

The gold films produced in this way were continuous and oriented epitaxially to the underlying rock salt. Figure 3A and B shows the TEM image and the diffraction pattern of a 350Å film. It shows that the film was a single crystal oriented with the <100> plane parallel to the film plane. Defects in the film include pinholes (100Å wide) and microtwins typical of such films (12).

The polymer solutions were 1 weight percent (w/o) PEO in aceotnitrile and had a monomer to Ag^+ ratio of 10 to 1. The solutions were applied to the gold working electrodes using a microsyringe having a glass tip; generally between 2 and 4 μl were applied. Solvent evaporation was accomplished in air or by heating at ~50°C in a vacuum oven for about 10 min.

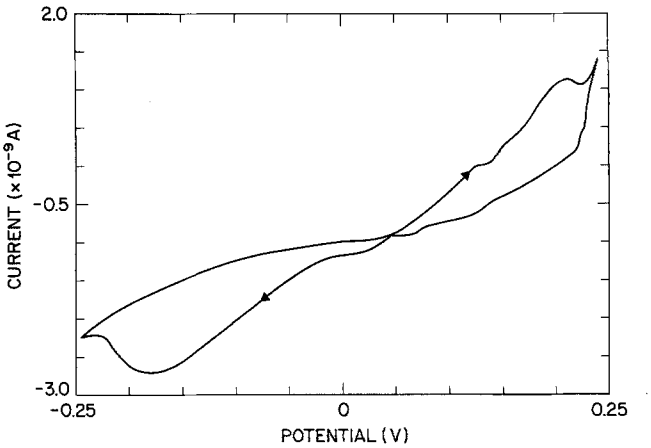

Fig. 5. Cyclic voltammogram of $AgBF_4$/PEO thin cell taken in microscope cartridge at 40°C. Thickness of cell is approximately 150Å.

The silver anode was made by evaporating silver onto the polymer-coated gold layer on the rock salt in the same bell jar evaporator at room temperature. The silver film is of similar thickness to the gold but is polycrystalline with small grains (~100Å) due to the low deposition temperature and the presence of a disordered polymer film on the substrate. The cells were transferred to a TEM grid by floating from the rock salt onto the surface of water and "netting" them with a TEM grid. Figure 4 shows that diffraction pattern from the total cell. The gold <100> spots are still visible, and the polycrystalline silver appears as rings around the center diffraction spot.

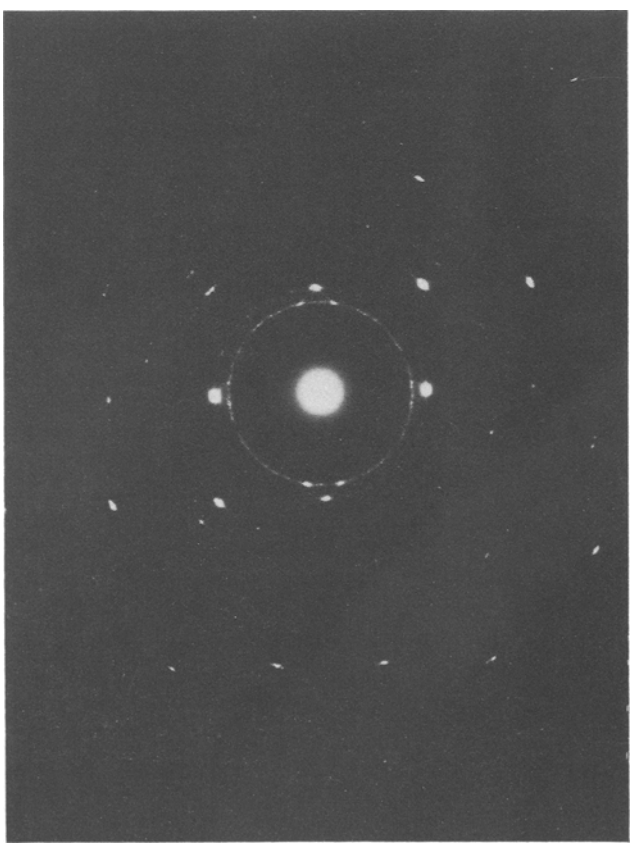

Fig. 4. Diffraction pattern from cell, including gold film, polymer layer, and silver film.

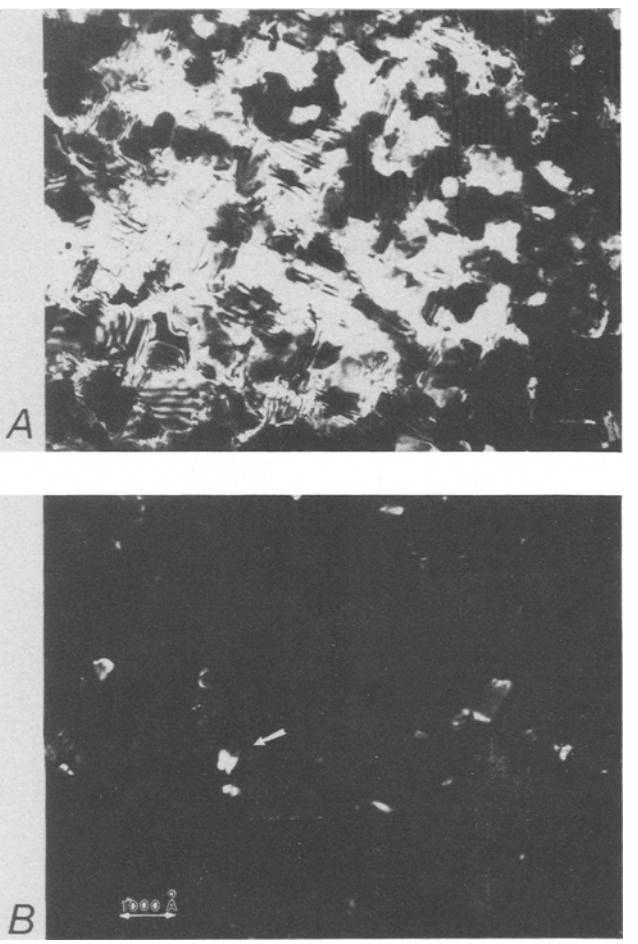

Fig. 6. Dark field images from gold <200> spot in the *in situ* cell. The bright area shows the gold film clearly (A), but misoriented silver crystallites (arrow) are visible where the gold is bent away from the Bragg condition (B).

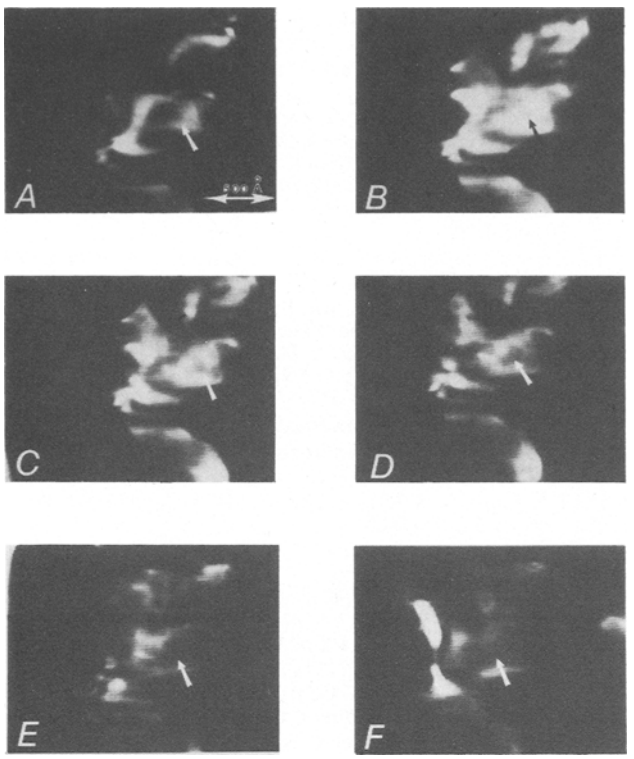

Fig. 7. Dark field images (gold <200>) taken sequentially in an *in situ* deposition experiment. Arrows show growth and coalesence of silver islands.

Microscope.—The instrument used was a modified JEOL 200CX operated at 200 kV (14). The cell is held in place in the cartridge with tantalum clips that make electrical contact to the electrodes in the cell. The top-entry cartridge does not allow specimen tilting. Images were recorded either on photographic plates or on a Nd:YAG scintillator and TV camera (Gatan, Incorporated) for dynamic recording, from which Polaroid copies have been made.

Images are taken using diffraction contrast which is sensitive to specimen thickness, orientation, and defects. In <200> dark-field images, which monitor only the scattered electrons from the <200> planar spacing in gold, we can directly observe the gold substrate and any deposited silver which grows epitaxially, without significant contrast from misoriented grains in the silver electrode or the disordered polymer (which scatter into other parts of the diffraction pattern).

Results.—Cyclic voltammetry experiments analogous to those shown in Fig. 2 for the thicker "swagelok cells" were performed on the thin cells in the microscope cartridge. Figure 5 shows results obtained at 40°C for a cell having a $AgBF_4$/PEO electrolyte. For the most part the details of the cyclic voltammetric behavior obtained in the larger swagelok cells were reproduced with the thin cells in the microscope. Nevertheless, since making robust connections to the thin metal electrodes was the most difficult step of experiment, we sometimes observed partial shorting in the cell from poor clip connections. However, even under these conditions, the TEM observations were consistent with electrochemical deposition of silver.

Figure 6a and b are dark field images from a <200> gold diffraction spot taken from the cell containing $AgAsF_6$ electrolyte. The twin boundaries in the gold film are indicated by moiré patterns. In a different area of the same cell, shown in part b, the surface of the gold is bent in such a way that the Bragg condition is not met (so the gold film appears dark) but misoriented silver grains can be seen (marked by arrow).

When the cell is polarized cathodically (*vs.* the silver anode), changes in the gold dark field image start to appear. Figure 7 shows a series of images taken sequentially in an *in situ* deposition experiment with a <200> gold reflection. This image would show gold and oriented silver which may grow epitaxially. During the experiment the cell was polarized from 0 V to −600 mV at a rate of 10 mV/s, but because the cell became partially shorted it was not possible to monitor the total current through the cell. The images show the formation and growth of epitaxial islands on the gold film in the thin regions of the cell between the silver grains (noted by the arrows in Fig. 7 A-F). These are tentatively identified as silver islands which grow in diameter and coalesce to form extended deposited layers. At longer times (Fig. 7F) the image becomes substantially darker, consistent with thickening of the deposited layer.

A second type of deposited structure was observed in the *in situ* experiments. Bright field images of the cell taken after passage of considerable charge (Fig. 8) showed borders around the dark silver grains which continued to grow in thickness as long as the cell was polarized. These growing layers can be attributed to silver deposition beneath the silver grains onto the nearby gold film.

TEM diffraction contrast imaging is readily able to resolve thickness changes associated with deposition of as little as 20Å. With controlled diffraction conditions this thickness can be measured absolutely (15). Using special Bragg reflections it has been possible to resolve monatomic steps on the surface of silver or gold films (16). A major feature of the TEM technique in this respect is that such imaging can equally well be performed at a buried interface, provided the background scattering from disordered material (*i.e.*, a polymer layer) is sufficiently low. For this reason we will attempt to operate these cells with the thinnest possible polymer layers. The interaction of the growing film with defects in the substrate, and the introduction of defects into the films to relieve misfit stress, will be easily observable.

Conclusions

Preliminary results are given which describe electrochemical deposition and stripping behavior of silver from

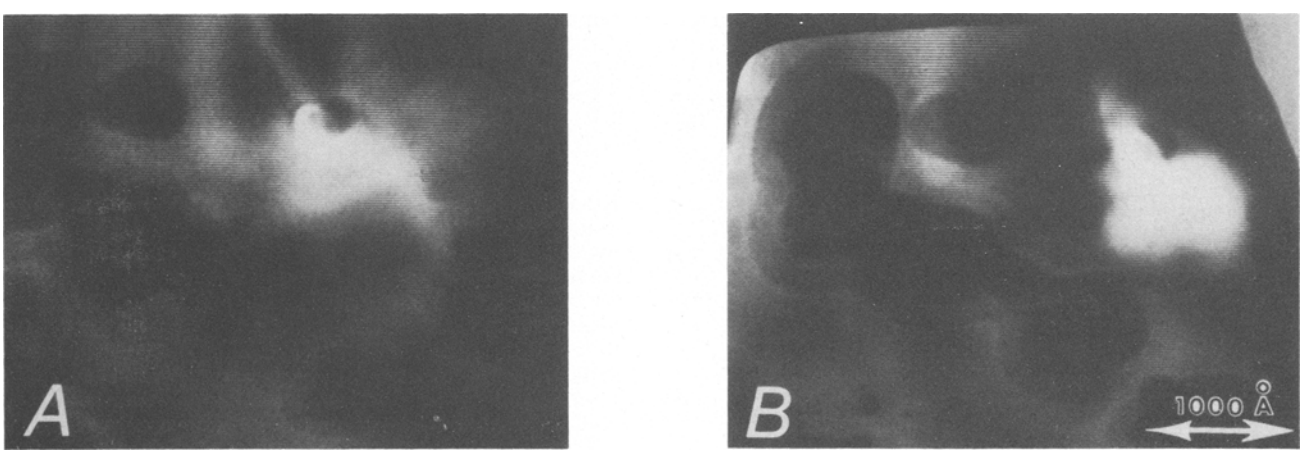

Fig. 8. Bright field images taken during *in situ* deposition experiment. Borders (arrow) near silver grains are not seen before passage of current.

a Ag/PEO(Ag^+)/Au cell, and the direct observation by TEM of electrochemically deposited silver from a very thin cell of the same composition. Cyclic voltammetry experiments show that silver can be deposited and stripped from gold substrates using a polyethylene oxide/$AgAsF_6$ electrolyte, provided that the temperature is above about 35°C. By polarizing the cell in the TEM, epitaxial deposition was observed to occur by island nucleation, growth and coalescence. It appears that the process is complicated and that more than one growth mechanism is operative. Although experimental problems to reliably make contact to the films without shorting have not yet been entirely overcome, this problem should be solvable. The development of a technique to directly observe the early stages of nucleation and growth of electrodeposited films by TEM, combined with conventional electrochemical methods will allow the possibility of investigating the structure of electrodeposits on an atomic level.

Acknowledgments

We would like to thank Frank Unterwald for the use of his evaporator, Ed Reitman for making the conductivity measurements, and Charlie Mattoe for plating the TEM grids.

Manuscript submitted June 9, 1988; revised manuscript received Feb. 27, 1989. This was Paper 535 presented at the Atlanta, GA, Meeting of the Society, May 15-20, 1988.

AT&T Bell Laboratories assisted in meeting the publication costs of this article.

REFERENCES

1. See for example, "Electrocrystallization," R. Weil and R. G. Barradas, Editors, The Electrochemical Society Softbound Proceedings Series, PV 81-6, Pennington, NJ (1981).
2. B. E. Fenton, J. M. Parker, and P. V. Wright, *Polymer*, **14**, 589 (1973).
3. M. Armand, J. M. Chabango, and M. Duclot, in "Fast Ionic Transport in Solids," P. Vashijhta, J. N. Mundy, and G. K. Shenoy, Editors, p. 131, North-Holland, New York (1979).
4. S. Swathirajan and S. Bruckenstein, *This Journal*, **129**, 1202 (1982).
5. S. Swathirajan and S. Bruckenstein, *J. Phys. Chem.*, **86**, 2480 (1982).
6. L. S. Melnick, T. M. Riedhammer, and S. Bruckenstein, in "Electrode Processes 1979," S. Bruckenstein, J. D. E. McIntyre, B. Miller, and E. Yeager, Editors, p. 306, The Electrochemical Society Softbound Proceedings Series, PV 80-3, Princeton, NJ (1980).
7. S. T. Rao, R. Weil, *This Journal*, **127**, 1030 (1980).
8. S. T. Rao, and R. Weil, *Trans. Inst. Metal Finish.*, **57**, 97 (1979).
9. M. L. Kaplan, E. A. Rietman and R. J. Cava, *Solid State Ionics*, **17**, 67 (1985).
10. P. C. Andricacos and P. N. Ross, *This Journal*, **130**, 1340 (1983).
11. R. F. Adamsky and R. E. LeBlanc, *J. Vac. Sci Technol.*, **2**, 79 (1965).
12. J. W. Mathews, *Appl. Phys. Lett.*, **7**, 131 (1965).
13. D. W. Pashley, *Advan. Phys.*, **5**, 173 (1956).
14. M. L. McDonald, J. M. Gibson, and R. C. Unterwald, *J. Sci. Inst.*, To be published.
15. P. B. Hirsch, A. Howie, R. B. Nicholson, D. W. Pashley, and M. J. Whelan, "Electron Microscopy of Thin Crystals," R. Kreiger, Malabar, FL (1977).
16. D. Cherns, *Phil. Mag.*, **30**, 549 (1974).

A Study of Contact Angle of Hydrogen Bubbles Formed by Formaldehyde Oxidation on Copper Electrode

H. H. Trieu and R. R. Chandran*,[1]

Department of Chemical Engineering, University of Akron, Akron, Ohio 44325

R. F. Savinell*

Department of Chemical Engineering, Case Western Reserve University, Cleveland, Ohio 44106

ABSTRACT

During electroless copper deposition, the hydrogen bubbles formed by formaldehyde oxidation affect the quality of the product plate. Photographic and electrochemical studies were carried out to obtain information on contact angle of hydrogen bubbles evolving from a miniature copper electrode. In general, the contact angle is related inversely to the bubble diameter. For the concentration range of the electrolyte used in this study, the contact angle is not significantly affected by the pH, agitation, and concentrations of formaldehyde, complexing agents (EDTA and QUADROL) and surfactant (sodium dodecyl benzene sulfonate). However, these components and their concentration did affect other characteristics such as growth rate, detachment diameter, and population density of hydrogen bubbles.

The electroless copper plating technique is widely applied in the manufacturing of printed circuit boards. The kinetics of electroless copper deposition has been investigated (1-4), and the overall reaction can be written as (1)

$$Cu^{++} + 2HCHO + 4\,OH^- \rightarrow Cu + H_2 + 2H_2O + 2HCOO^- \quad [1]$$

This overall reaction takes place as the following two local electrochemical half reactions:

Formaldehyde oxidation

$$2HCHO + 4\,OH^- \rightarrow 2HCOO^- + 2H_2O + H_2 + 2e^- \quad [2]$$

Cupric reduction

$$Cu^{++} + 2e^- \rightarrow Cu^o \quad [3]$$

During electroless copper deposition, liquid in the immediate vicinity of the solid surface becomes highly supersaturated with the hydrogen product. Some of the dissolved hydrogen product is transported to the liquid bulk by molecular diffusion and liquid convection. Also, phase transformation takes place at nucleation sites when the liquid adjacent to the surface becomes sufficiently supersaturated. The hydrogen bubbles adhering to the surface then grow by mass diffusion from the surrounding liquid and sometimes by coalescing with nearby growing bubbles. The bubbles eventually detach from the surface when they reach a size at which the buoyancy forces plus

* Electrochemical Society Active Member.
[1] Present address: Pitt Metals and Chemicals, McDonald, Pennsylvania 15057.